Nanoscale

Accepted Manuscript

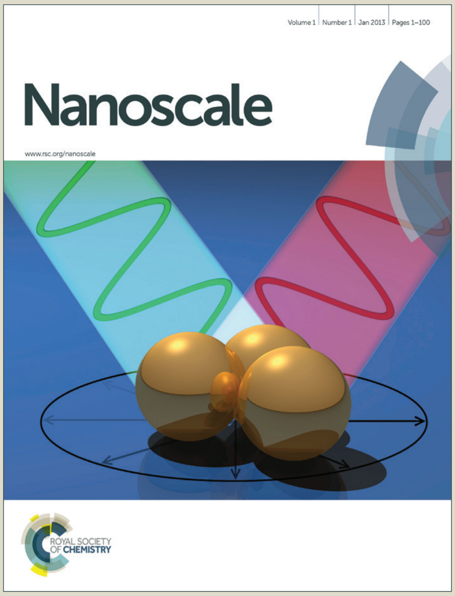

ROYAL SOCIETY OF CHEMISTRY

www.rsc.org/nanoscale

Enhanced photocatalytic response of nanometric TiO_2 wrapping Au nanoparticles for eco-friendly water applications

Viviana Scuderi,[a] **Giuliana Impellizzeri,**[a*] **Lucia Romano,**[a,b] **Mario Scuderi,**[c] **Maria V. Brundo,**[d] **Kristin Bergum,**[e] **Massimo Zimbone,**[a] **Ruy Sanz,**[a] **Maria A. Buccheri,**[a] **Francesca Simone,**[b] **Giuseppe Nicotra,**[c] **Bengt G. Svensson,**[f] **Maria G. Grimaldi,**[a,b] **and Vittorio Privitera**[a]

(a) CNR-IMM MATIS, Via S. Sofia 64, I-95123 Catania, Italy

(b) Department of Physics and Astronomy, University of Catania, Via S. Sofia 64, I-95123 Catania, Italy

(c) CNR-IMM, Z.I. VIII Strada 5, 95121 Catania, Italy

(d) Department of Biological, Geological and Environmental Sciences, University of Catania, Via Androne 81, 95124, Catania, Italy

(e) Department of Chemistry, Centre for Materials Science and Nanotechnology, University of Oslo, P. O. Box 1033, Blindern, N-0315 Oslo, Norway

(f) Department of Physics, Centre for Materials Science and Nanotechnology, University of Oslo, P. O. Box 1048, Blindern, N-0318 Oslo, Norway

* **Corresponding Author:** giuliana.impellizzeri@ct.infn.it

Abstract

We propose a ground-breaking approach by an upside-down vision of the Au/TiO_2 nano-system in order to obtain an enhanced photocatalytic response. The system was synthesized by wrapping Au nanoparticles (~ 8 nm mean diameter) with a thin layer of TiO_2 (~ 4 nm thick). The novel idea of embedding Au nanoparticles with titanium dioxide takes advantage of the presence of metal nanoparticles, in terms of electron trapping, without losing any of the TiO_2 exposed surface, so to favor the photocatalytic performance of titanium dioxide. A complete structural characterization was made by scanning electron microscopy, transmission electron microscopy and X-ray diffraction. The remarkable photocatalytic performance together with the stability of the nano-system were demonstrated by the degradation of Methylene blue dye in water. The non-toxicity of the nano-system was established by testing the effect of the material on the reproductive cycle of *Mytilus galloprovincialis* in an aquatic environment. The originally synthesized material was also compared to conventional TiO_2 with Au nanoparticles on top. The latter system showed a dispersion of Au nanoparticles in the liquid environment, due to their instability in the aqueous solution that clearly represents an environmental contamination issue. Thus, the results show that nanometric TiO_2 wrapping of Au nanoparticles has a great potential in eco-friendly water/wastewater purification.

KEYWORDS: TiO_2, Au nanoparticles, water, photocatalysis, toxicity

Introduction

Today, one of the biggest problems of humanity is the inadequate access to clean water. This problem is expected to grow in the coming years, when water scarcity will be global, even in regions currently considered water-rich. For this reason, much effort is devoted to study new methods of purifying water, efficiently, with less energy, also minimizing the consumption of chemical compounds and their impact on the environment.

Since photo-induced decomposition of water on TiO_2 electrodes was discovered,[1] semiconductor-based photocatalysis has attracted extensive interest. One particular focus has been on mineralization and disinfection of water.[2-7]

TiO_2 (commonly called *titania*) is efficient, harmless, stable and inexpensive, thus limiting the choice of convenient alternatives.[8] When TiO_2 is irradiated with photons of energy equal to or higher than its band-gap (3.15 eV for anatase, 3.05 eV for rutile crystalline phase[9]), the generated electron–hole pairs can induce on its surface (in contact with water) the formation of reactive oxygen species (ROS), such as $OH\cdot$, which are directly involved in the oxidation processes that remove persistent organic compounds and microorganisms in water. In particular, the holes are responsible for the hydroxyl radicals ($OH\cdot$) production, by a chemical reaction with the H_2O molecules. The use of TiO_2 nanoparticles for this purpose has demonstrated successful results. However, its main technical barrier hindering its commercialization at an industrial scale is the cost of separating TiO_2 particles from water after the treatment.[10] In fact, the permanency of photocatalytic powder in the solution requires other successive filtration and/or centrifugation steps, increasing the impossibility or difficulty to reuse the same photocatalyst more than once. In order to overcome these problems, recent investigations are oriented toward the photocatalyst immobilization in the form of film.[11-13] The studies reported in the literature usually employ thick films; for example in Ref. 12 the authors prepared by sol-gel deposition a TiO_2 layer with a thickness of 0.7 μm. A recent work experimentally quantified the charge diffusion length in high-quality epitaxial titania: 3.2 nm for the anatase phase, 1.6 nm for the rutile phase, showing that a surface region of a few nanometer depth provides charge carriers for photoreactions.[14] This clearly means that the use of a thick film is useless. Another limiting factor of TiO_2 is that the photogenerated electron-hole pairs undergo fast recombination, lowering the efficiency of the photocatalytic process. Such an undesired effect can be reduced by placing noble metal nanoparticles on top of the TiO_2 semiconductor surface. Thanks to the formation of a Schottky junction at the metal/semiconductor interface, electrons can be efficiently trapped by noble metals,[15] enhancing the electron-hole separation. Among the different metals, gold nanoparticles have been widely used to enhance the efficiency of TiO_2, due to the system's excellent ability for photocatalytic degradation of several pollutants.[15-16] Most of the literature is focused on the photocatalytic gold/titania colloids (see for example Refs. 17-19), and only a few deal with thin film surfaces (see for example Refs. 16, 20). Moreover, it is now well established that in the case of gold particles deposited on top of the titania, the photocatalytic efficiency of the system is driven by a compromise between the Au action in capturing the electrons and the coverage of the TiO_2 surface resulting from the presence of gold particles, that negatively affect the photocatalytic performance of the material.[21,22] In addition, with the growing use of nanotechnology, the safety of nanomaterials and their potential impact on the environment has become a critical issue. Indeed, the implementation of nanomaterial-based technologies could result in the release of nanomaterials in the environment, via the contact of nanostructured materials with the treated water.[23]

In order to meet the technological requirements, we developed an innovative TiO_2/Au nano-composite synthesized by sputtering and atomic layer deposition (ALD) techniques. The peculiarity of the system is the wrapping of gold nanoparticles (~ 8 nm mean diameter) with a thin layer of TiO_2 (~ 4 nm thick). The ALD technique is one of the few techniques able to realize films with a controlled thickness of few nanometers, that effectively contribute to the photoreactions,[14] avoiding any wastefulness of material. This optimized design takes advantage of the presence of metal nanoparticles (in terms of electron trapping), without losing any TiO_2 exposed surface. In addition, the form of thin film eliminates the problem of a particle filtration step after the water treatment.

The present work is devoted to the investigation of the photocatalytic activity along with the stability of the synthesized TiO_2/Au nano-system. Special attention has been paid to the toxicity of the nano-composite by testing the reproductive cycle of *Mytilus galloprovincialis,* that is a suitable animal model for environmental toxicology studies of nanoparticles.[24] In addition, the synthesized material was compared both to a TiO_2 flat film and to conventional TiO_2 with Au nanoparticles on top.

Experimental

A gold film, with a thickness of ~ 5 nm, was sputtered on a quartz substrate. In order to induce the self-organization of the metal nanoparticles, the samples were annealed at 600°C for 1 h in a conventional furnace under a controlled N_2 flux. The as-synthesized gold nanoparticles (~ 8 nm mean diameter) were covered with a thin layer of TiO_2 (~ 4 nm thick), deposited by ALD. Since the ALD process is intrinsically atomic, ALD produces layers with nanometer scale thickness control.[25,26] The ALD was performed with a Beneq TFS-200 system, with $TiCl_4$ (Sigma Aldrich, 99.9%) and de-ionized water as precursors, at a deposition temperature of 200 °C. Nitrogen (> 99.999%) from a Sirocco N_2 generator was used as carrier gas, with a combined flow rate of 550 sccm, maintaining a reactor pressure of approximately 1.3 mbar. The deposition of the TiO_2 film on top of the gold nanoparticles avoided the photocatalytic efficiency loss due to coverage of the TiO_2 surface by the metal particles (see for example Refs. 21, 22). This sample typology will be hereafter called “TiO_2/Au” (i.e. TiO_2 on Au nanoparticles). Two reference samples were also synthesized and used for comparison: 1) a TiO_2 flat film (~ 4 nm thick) deposited by ALD on a quartz substrate, hereafter simply called “TiO_2”; 2) Au nanoparticles on top of TiO_2 film (~ 4 nm thick), realized by ALD and sputtering, on a quartz substrate, that is the configuration commonly reported in the literature (see for example Refs. 21, 22), hereafter called “Au/ TiO_2” (i.e. Au nanoparticles on top of the TiO_2).

The structural characterization was performed by scanning electron microscopy (SEM), transmission electron microscopy (TEM) and X-ray diffraction (XRD). SEM analyses were performed in plan-view by a field emission Zeiss Supra 25 microscope. TEM analyses were performed in cross-section by a JEOL JEM-2010F microscope operated at 200 KeV and equipped with a post-column Gatan GIF 2001 energy image filter. XRD measurements were acquired by a Bruker D-500 diffractometer at several angle of incidence, from 0.8 to 1.0º, and Θ-2Θ from 20 to 60º. Acquired spectra were analyzed by a Bruker software suite, including ICSD structure database.

The optical characterization was obtained by extracting both the total transmittance (T) and the total reflectance (R) spectra in the 200-800 nm wavelength range, by using a Varian Cary 500 double beam scanning UV/Vis/NIR spectrophotometer equipped with an integrating sphere.

The photocatalytic activity of the investigated materials was evaluated by the degradation of the Methylene blue (MB) organic compound. The samples, 1 cm × 1 cm in size, were immersed in a solution (2 ml) containing MB and de-ionized water (starting concentration: 1.5×10^{-5} M). The mixture was irradiated by an UV lamp (peaked at 365 nm with 20 nm of full width at half maximum) with a irradiance of 1.1 mW/cm^2 for a total time of 3.5 hours. Every 15 minutes of irradiation and every 30 minutes after a total time of 1 hour, the solution was measured with an UV-VIS spectrophotometer (Perkin-Elmer Lambda 35) in a wavelength range between 500 and 800 nm. The degradation of MB was evaluated by the absorbance of the MB peak at 664 nm, using the Lambert-Beer law[27] ($A = \varepsilon \times l \times C$, where A is the absorbance of the solution at 664 nm, ε is the molar extinction coefficient, l is the width of the cuvette, C is the concentration of the MB). The UV lamp used for the irradiation does not emit in the region of absorption of the MB, as a consequence the measured degradation of the MB can be only ascribed to the presence of the catalyst. The decomposition of the MB in the absence of any catalyst materials was also checked as a reference. Before the measurements, the samples were irradiated by the UV lamp for 30 min in order to remove the hydrocarbons localized on the sample surface.[28] The stability of the nano-systems was checked by repeating seven times the MB degradation measurements. In detail, at the end of each experiment, the samples were washed and left immersed in de-ionized water for 15 h, in order to remove possible residues of the MB and to test the stability in an aqueous environment.

The toxicity of the synthesized TiO_2/Au nano-composite was tested by the reproductive cycle of *Mytilus galloprovincialis*. Adults were cleaned and stored at 4 °C until testing. The spermiotoxicity test was performed according to the method proposed by His *et al.*[29], on the basis of the standard protocol of US EPA (1995).[30] Adults were induced to spawn by thermal stimulation (temperature cycles at 18 and 28 °C). Gametes of good quality derived from the best males and females were selected and filtered at 32 µm (sperms) and 100 µm (eggs), in order to remove impurities. Eggs (1000 ml) were fertilized by injecting 10 ml of sperms, and fecundation was verified by light microscopy. Egg density was determined by counting four subsamples of known volume. Fertilized eggs, added to test solutions in order to obtain a density of 10–20 eggs ml^{-1}, were incubated for 24 h at room temperature in 5 ml of salt water on the surface of the TiO_2/Au samples. The reliability of the results was based on the evaluation of control samples. Five replicates for each sample were tested. The toxicity of free commercial Au nanoparticles in salt water solution was also tested in order to discriminate the eventual impact of the stable nano-composite and of free nanoparticles.

Results and discussion

Figure 1 shows the two final steps of the synthesis process of the TiO_2/Au nano-system, together with the morphological and structural characterization. In particular, Fig. 1 (b) reports a plan-view SEM image of the Au nanoparticles on the quartz substrate, just after the thermal treatment (the schematic of the sample is shown in Fig. 1 (a)). The size distribution of the nanoparticles was calculated by a Gatan Digital Micrograph program, taking into account several micrographs, about 1700 nm × 1200 nm in size, each containing ~ 2000 nanoparticles. The sample is composed by a homogeneous distribution of gold nanoparticles with an average diameter of ~ 8 nm. Figure 1 (d) shows a cross-section energy filtered-transmission electron microscopy (EF-TEM) image after the deposition of the TiO_2 layer by ALD (the schematic of the sample is shown Fig. 1 (c)). EF-TEM image is in false colors and was obtained by filtering the energy loss for the electrons at 35 eV corresponding the Ti-$M_{2,3}$ atomic edge. The resulting Ti containing layer is reported in magenta, while the Au nanoparticles are in black. The image clearly shows the presence of a thin and continuous titanium dioxide film, ~ 4 nm in thickness, wrapping the Au nanoparticles. TEM analyses also reveal that, even though the Au nanoparticles are well covered by the titania film, there is not a significant increase of the TiO_2 exposed surface due to the presence of nanoparticles underneath (see Fig. 1 (c)).

XRD measurements of TiO_2 films (50 and 100 nm in thicknesses), deposited by ALD with the same experimental conditions of the 4 nm thick film reported in this paper, revealed that the deposited polycrystalline TiO_2 is in the anatase phase, as confirmed by the diffraction pattern obtained during the TEM analyses of the 4 nm thick film. This result is in perfect agreement with what is reported in the literature for ALD deposition at 200 °C, using $TiCl_4$ as precursor.[31,32]

Figure 2 displays the absorbance (A) of the TiO_2/Au sample, obtained by the transmittance (T) and reflectance (R) spectra (A = 1 - T - R). The material shows a significant light absorption at ~ 600 nm, that is the typical Plasmon resonance of gold containing samples[33] and an absorption band in the UV part of the spectrum (from 350 nm towards shorter wavelengths). The latter absorption band is related to the titania film. The optical band-gap of the TiO_2 was evaluated by applying the Tauc model.[34] According to the Tauc law:

$$\alpha = \frac{B}{h\nu}(h\nu - E_{gap})^2 \qquad (1)$$

where α is the absorption coefficient, B is the Tauc constant,[35] $h\nu$ is the incoming photon energy, while the E_{gap} is the optical band-gap of the material. The absorption coefficient, α, was extracted from the transmittance and reflectance measurements by using the following equation:

$$\alpha = \frac{1}{d_f}\ln\frac{T_Q(1-R_f)}{T_f} \qquad (2)$$

where d_f is the thickness of the film, T_Q is the transmittance of the quartz substrate, R_f and T_f are, respectively, the reflectance and the transmittance of the investigated film. From the inset of Fig. 2 it can be seen that the E_{gap} value (intercept of the linear fit with the energy axis) is 3.0 eV. Assuming an error of ~ 10%, this value is in perfect agreement with the value of 3.15 eV reported in the literature for bulk anatase TiO_2.[9] An optical energy gap of 3.2 eV was obtained with the same procedure for the reference TiO_2 flat film (not shown).

The photocatalytic activity in the degradation of an organic compound dissolved in water under UV irradiation was checked by Methylene blue. Figure 3 illustrates a typical measurement of MB discoloration. In more detail, Fig. 3 reports the absorption spectra for the MB solution for different irradiation time for the TiO_2/Au samples. The absorbance peak at 664 nm is a direct measurement of the MB concentration (through the Lambert-Beer law[27]) and thus its decrease with UV irradiation time is a measure of the photocatalytic decomposition of the MB molecules.

The photocatalytic response of the TiO_2/Au sample was compared to two reference samples: 1) TiO_2 flat film (~ 4 nm thick) deposited on a quartz substrate; 2) Au/TiO_2, i.e. Au nanoparticles on top of the TiO_2 film (~ 4 nm thick) deposited on a quartz substrate, that is the configuration commonly reported in the literature (see for example Refs. 21, 22). The first test was performed under dark condition for 12 hours, in order to evaluate the degree of adsorption of the MB on the beaker walls and on the three types of samples. The beaker walls showed an adsorption of ~ 3%, while the samples showed an adsorption of ~ 1% (reaching these maximum values after 30 min). This latter result indicates that the investigated materials do not adsorb the MB, since the adsorption value of 1% is equal to the experimental error of the discoloration measurements. Figure 4 reports the residual concentration of the MB: C/C_0, where C is the concentration of the MB after the irradiation, C_0 is the starting concentration of the MB, versus the irradiation time. We tested four samples: MB in the absence of any catalyst materials (squares), MB with the TiO_2 sample (circles), MB with the Au/TiO_2 sample (triangles) and MB with the TiO_2/Au sample (diamonds). It is important to underline that the discoloration measurements are not repeatable during the time, due to the slight variation of the lamp power and of the starting concentration of the MB. As a consequence, a rigorous method to analyze the experimental data is to compare the measurements simultaneously(i.e. samples immersed in the same as-prepared MB/de-ionized water solution and simultaneously irradiated with the UV lamp); the comparison between data obtained in different days can be done taking into account the relative difference, and not the absolute values obtained for the different catalyst materials. This rigorous method has been applied for the presented work. Fig. 4 (a) shows a reduction of the MB concentration (squares) of about 5% in 210 min, due to adsorption effects of the beaker walls. A more significant decrease in the MB concentration is clearly observed when the photocatalytic materials are added to the solution. A photocatalytic activity is evidenced for the TiO_2 flat film (see circles in Fig. 4 (a)). It is interesting that the Au/TiO_2 sample has a photo-response almost equal, within the experimental errors, to the TiO_2 sample. This results can be understood considering the excessive coverage of the TiO_2 surface by the Au nanoparticles. Indeed, a surface coverage of about 35% (with an error of 2%) was estimated by plan-view SEM analysis, using the Gatan Digital Micrograph program. This value is in perfect agreement with the result of Armelao *et al.*[22], where a surface coverage of about 32% by gold did not result in a beneficial effect on the photocatalytic activity of titania. The TiO_2/Au system instead exhibits a remarkable increase in MB degradation by more than 10%, after 210 min, compared to the TiO_2 sample (compare diamonds to circles in Fig. 4 (a)). It is worth noting that a reduction of the MB by 26% compared to the starting concentration of the MB (i.e. $C/C_0 = 0.74$ in 210 min, see Fig. 4 (a)) is a remarkable value considering the size of the samples and the power of the lamp. Indeed, we used samples 1 cm × 1 cm in size so as to perform the UV irradiation of the different samples simultaneously; a UV lamp power of 8 W assured no evaporation of the solution; the starting concentration of the MB was fixed by the literature. Obviously, with larger samples and by a more powerful lamp we would have obtained a higher reduction of the MB.[4]

In order to test the stability of the investigated materials we repeated the photo-degradation measurements up to seven times. Figure 4 (b) and (c) reports the results for the fourth and the seventh process, respectively. Repeating the experiment up to seven times, we observed that the improvement of the MB degradation of the TiO_2/Au samples, with respect to the TiO_2 film is quite constant at ~ 10% (see Fig. 4 (a), (b) and (c)). It is worth noting, as said before, that the comparison between data obtained in different days can be only done taking into account the relative difference. So we can affirm that the TiO_2/Au nano-system presents a very stable response without significant efficiency loss. Opposite results were obtained for the conventional Au/TiO_2 samples. Fig. 4 (a), (b) and (c) show a remarkable change in the photocatalytic activity of the system. In detail, while at the beginning the MB degradation is almost equal to the one of the TiO_2 sample (see Fig. 4 (a)), it increases with time: 3% and 8% for the fourth and the seventh experiment, respectively. The observed trend can be explained by the dispersion of the Au nanoparticles in the liquid environment, due to their instability in the aqueous solution. In fact an inhibition of the gold action in capturing electrons is its coverage of the titania surface, that means less titania surface is directly exposed to the irradiation and is available for light and pollutant adsorption.[21,22] The photocatalytic efficiency of the system is indeed driven by a compromise between the Au action in capturing the electrons and the screening resulting from the presence of gold on the titania surface, that negatively affects the photocatalytic performance of the material.[21,22] The instability of Au nanoparticles in the liquid environment was confirmed by an accurate analysis of the SEM images of the Au/TiO_2 samples. The analyses indicated a reduction of the TiO_2 coverage from 35% to 29% from the first to the seventh process. Thus, the time in the liquid environment induced a detaching of Au nanoparticles from the TiO_2 surface, causing as a consequence an increase of the photocatalytic efficiency. However, the Au/TiO_2 system is unstable and the presence of Au residuals can represent a water contamination issue.

The experimental results indicated a strong instability of the conventional Au/TiO_2 nano-system, whereas the TiO_2/Au nano-composite shows an excellent reproducibility of the photocatalytic activity, with a remarkable ability in degrading the MB with respect to TiO_2 flat film.

According to the Lagmuir-Hinshelwood model, the photo-degradation reaction rate, *k*, of water contaminants is given by the following reaction:

$$\ln\left(\frac{C}{C_0}\right) = -kt \qquad (3)$$

where C is the concentration of organic species, C_0 is the initial concentration of organic species, t is the irradiation time.[4] We report in Fig. 5 the photo-degradation rate for the first discoloration process (see Fig. 4 (a)). The rate for the different materials was normalized to the value obtained for the MB decomposition in the absence of any catalyst materials. In the abscissa axis "MB" indicates the MB decomposition in the absence of catalyst, that is 1 due to the normalization (i.e. k/k_{MB}); "TiO_2" refers to the MB decomposition in the presence of pure TiO_2 film, and so on for the other samples. Figure 5 shows a reaction rate of a factor of ~ 4 in the presence of TiO_2 flat film or Au/TiO_2 sample, and a higher rate of ~ 9 in the presence of TiO_2/Au sample. Thus, the TiO_2/Au sample exhibited a photo-degradation reaction rate that is ~ 2.5 times the rate of the TiO_2 flat film and Au/TiO_2 sample.

In order to check the potential use of the synthesized TiO_2/Au material in water treatment plants, we checked the eventual toxicity of the nanomaterial towards biological systems. Gold nanoparticles are known to be toxic. For example, Chao *et al.*[36] have demonstrated that Au nanoparticles induce acute inflammation and apoptosis in the mice liver; Tedesco *et al.*[24] have shown that Au nanoparticles produce significant lipid peroxidation in digestive glands of *Mytilus edulis*. The toxicity of the studied TiO_2/Au nano-system was evaluated by testing the effect of the material on the reproductive cycle of *Mytilus galloprovincialis* in an aquatic environment. This mollusk is widespread in marine environments, and it is considered an excellent biological indicator of marine pollution. The results of the experiment are reported in Fig. 6 by light microscope images. The analyses indicated that the sperms maintain good mobility up to 8 h (Fig. 6 (a)), while eggs do not show any morphological variation (Fig. 6 (b)). In addition, approximately 90% of the eggs had been fertilized after 15 minutes (Fig. 6 (c)). The development of the fertilized eggs was followed up to 24 h, revealing the absence of any anomalies in the first stages of the development, as indicated by the presence of numerous and normal blastulae clearly visible in Fig. 6 (d). This study demonstrates the non-toxicity of the TiO_2/Au sample. In addition, the results were compared with those obtained by monitoring the reproductive cycle of *Mytilus galloprovincialis* in the presence of free Au nanoparticles in solution, for three different solution concentrations: 10^9, 10^{10} or 10^{11} Au nanoparticles in 5 ml of salt water. For the highest amount of the Au nanoparticles a clear reduction of the spermatozoon mobility was visible. The obtained data agree with those present in the literature in which a decrease in sperm mobility has been demonstrated.[37,38]

Conclusions

We presented an experimental work focused on the photocatalytic efficiency and non-toxicity of the TiO_2/Au nano-system for water treatment. The system was originally synthesized by wrapping Au nanoparticles (~ 8 nm mean diameter) with a thin layer of TiO_2 (~ 4 nm thick), obtained by atomic layer deposition. The reported results show that the TiO_2/Au nano-system has a good efficiency in degrading the Methylene blue organic compound, an excellent stability in the water environment and a great reproducibility of its photocatalytic activity compared to the instability of the conventional Au/TiO_2 nano-system. In particular, the TiO_2/Au samples exhibited a photo-degradation reaction rate that is ~ 2.5 times the rate of the TiO_2 flat film and conventional Au/TiO_2 samples. The non-toxicity of the TiO_2/Au nano-system was established by testing the effect of the material on the reproductive cycle of *Mytilus galloprovincialis* in an aquatic environment. The results demonstrate that the originally-synthesized TiO_2/Au nano-system can be successfully implemented in water treatment plants.

Acknowledgment

The authors wish to thank F. Ruffino for fruitful discussion. This research has been supported by the FP7 European Project WATER (Grant Agreement 316082). TEM experiment were performed at

Beyondnano CNR-IMM, which is supported by the Italian Ministry of Education and Research (MIUR) under project Beyond-Nano (PON a3_00363).

References

1 A. Fujishima and K. Honda, *Nature*, 1972, **238,** 37.

2 D. F. Ollis, *Environ. Sci. Technol.*, 1985, **19**, 480.

3 S. Malato, P. Fernandez-Ibanez, M. I. Maldonado, J. Blanco and W. Gernjak, *Catal. Today*, 2009, **147**, 1.

4 M. N. Chong, B. Jin, C. W. K. Chow and C. Saint, *Water Res*., 2010, **44**, 2997.

5 W. Y.Teoh, J. A. Scott and R. Amal, *J. Phys. Chem. Lett*., 2012, **3**, 629.

6 R. Asahi, T. Morikawa, T. Ohwaki, K. Aoki and Y. Taga, *Science*, 2001, **293**, 269.

7 M. A. Shannon, P. W. Bohn, M. Elimelech, J. G. Georgiadis, B. J. Marinas and A. M. Mayes, *Nature*, 2008, **452**, 301.

8 T. L. Thompson and J. T. Yates Jr, *Chem. Rev*., 2006, **106**, 4428.

9 A. Bendavid, P. J. Martin, A. Jamting and Takikawa, *Thin Solid Films*, 1999, **355**, 6.

10 C. W. K. Chow and C. Saint, *Water Res*., 2010, **44,** 2997.

11 D. Byun, Y. Jin, B. Kim, J. K. Lee and D. Park, *J. Hazard. Mater*., 2000, **73**, 199.

12 M. C. Blount, D. H. Kim and J. L. Falconer, *Environ. Sci. Technol*., 2001, **35**, 2988.

13 Y. Zhang, J. Li and J. Wang, *Chem. Mater*., 2006, **18**, 2917.

14 T. Luttrell, S. Halpegamage, J. Tao, A. Kramer, E. Sutter and M. Batzill, *Sci. Rep*., 2014, **4**, 4043.

15 V. Subramanian, E. E. Wolf and P. V. Kamat, *J. Am. Chem. Soc*., 2004, **126**, 4943.

16 C. Yogi, K. Kojima, T. Hashishin, N. Wada, Y. Inada, E. Della Gaspera, M. Bersani, A. Martucci, L. Liu and T-K. Sham, *J. Phys. Chem. C*, 2011, **115**, 6554.

17 V. Subramanian, E. E. Wolf and P. V. Kamat, *Langmuir*, 2003, **19**, 469.

18 Z. Zheng, B. Huang, X. Qin, X. Zhang, Y. Dai and M-H. Whangbo, *J. Mater. Chem*., 2011, **21**, 9079.

19 N. Zhou, L. Polavarapu, N. Gao, Y. Pan, P. Yuan, Q. Wang and Q.-H. Xu, *Nanoscale*, 2013, **5**, 4236.

20 R.S. Sonawane and M.K. Dongare, *J. Molecul. Catal. A: Chem.*, 2006, **243**, 68.

21 I. M. Arabatzis, T. Stergiopoulos, D. Andreeva, S. Kitova, S. G. Neophytides and P. Falaras, *J. Catal.*, 2003, **220**, 127.

22 L. Armelao, D. Barreca, G. Bottaro, A. Gasparotto, C. Maccato, C. Maragno, E. Tondello, U. L. Stangar, M. Bergant and D. Mahne, *Nanotechnol.*, 2007, **18**, 375709.

23 H. Hillie and M. Hlophe, *Nature Nanotechnol.*, 2007, **2**, 663.

24 S. Tedesco, H. Doyle, J. Blasco, G. Redmond and D. Sheehan, *Aquat. Toxicol.*, 2010, **100**, 178.

25 N. Pinna and M. Knez, in *Atomic Layer Deposition of Nanostructured Materials*, ed. Wiley-VCH Verlag GmbH &Co. kGaA, Weinheim, Germany, 2012.

26 S. M. George, *Chem. Rev.*, 2010, **110**, 111.

27 A. D. McNaught and A. Wilkinson, in *Compendium of Chemical Terminology*, ed. Blackwell Scientific Publications, Oxford, 2nd ed. (the "Gold Book"), 1997.

28 R. Wang, K. Hashimoto, A. Fujishima, M. Chikuni, E. Kojima, A. Kitamura, M. Shimohigoshi and T. Watanabe, *Nature*, 1997, **388**, 431.

29 E. His, R. N. L. Seaman and R. Beiras, *Water Res.*, 1997, **31**, 351.

30 *Short-term methods for estimating the chronic toxicity of effluents and receiving waters to west coast marine and estuarine organisms*, EPA/600/R-95/136, Cincinnati, Ohio, USA, 1995.

31 J. Aarika, A. Aidla, H. Mandar and V. Sammelselg, *J. Crys. Grow.*, 2000, **220**, 531.

32 J. P. Lee, Y. J. Jang and M. M. Sung, *Adv. Funct. Mater.*, 2003, **13**, 873.

33 Y. Tian and T. Tatsuma, *J. Am. Chem. Soc.*, 2005, **127**, 7632.

34 J. Tauc, in *Amorphous and Liquid Semiconductors*, ed. by J. Tauc, Plenum, New York, 1974, p. 175.

35 S. Knief and W. von Niessen, *Phys. Rev. B*, 1999, **59**, 12940.

36 W.-S. Cho, M. Cho, J. Jeong, M. Choi, H.-Y. Cho, B.S. Han, S.H. Kim, H.O. Kim, Y.T. Lim and B.H. Chung, *Toxicol. Appl. Pharmacol.*, 2009, **236**, 16.

37 V. Wiwanitkit, A. Sereemaspun and R. Rojanathanes, *Fertil Steril.*, 2009, **91** 7.

38 U. Taylor, A. Barchanski, W. Garrels, S. Klein, W. Kues, S. Barcikowski and D. Rath, *Adv. Exp. Med. Biol.*, 2012, **733**, 125.

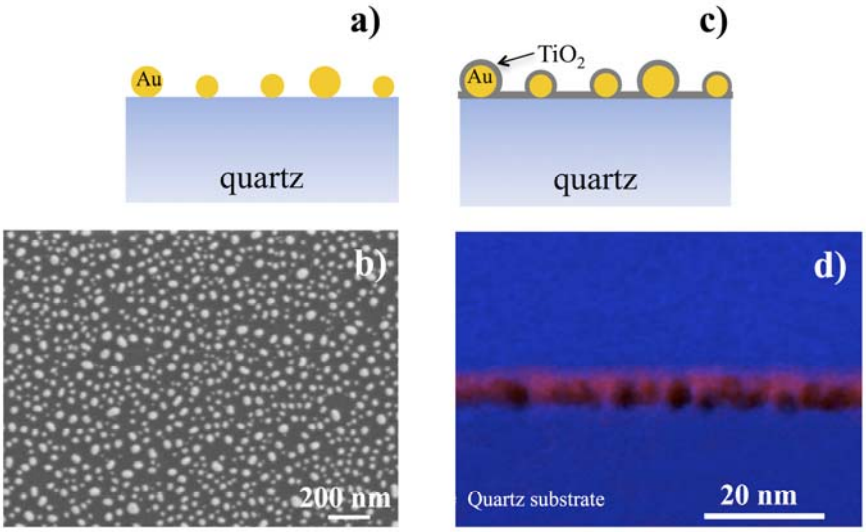

Figure 1: (a) scheme of the Au nanoparticles on the quartz substrate just after the thermal process, and (b) relative plan-view SEM image. (c) Scheme of the sample after the TiO_2 deposition by ALD, and (d) relative EF-TEM image in false colors (TiO_2 is reported in magenta, Au nanoparticles in black).

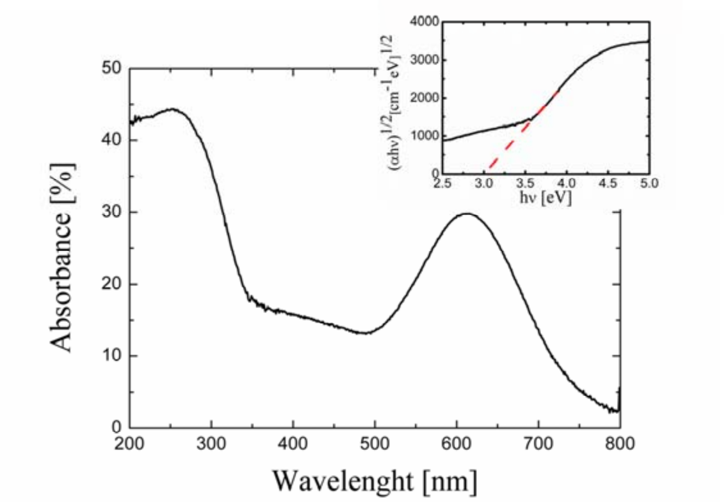

Figure 2: Absorbance spectrum of the TiO_2/Au sample. The inset shows the Tauc plot (continuous line) and the relative fit (dotted line) for the same sample.

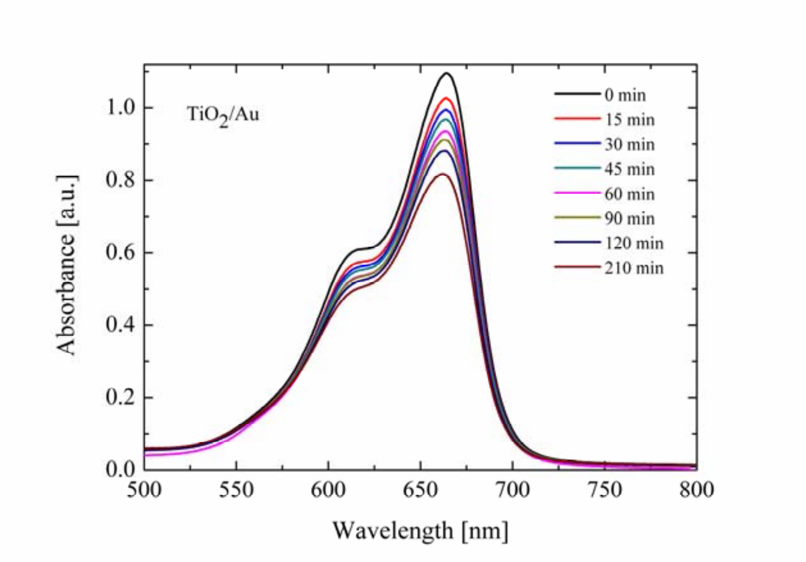

Figure 3: Absorption spectra for the MB solution for different irradiation times for the TiO_2/Au sample.

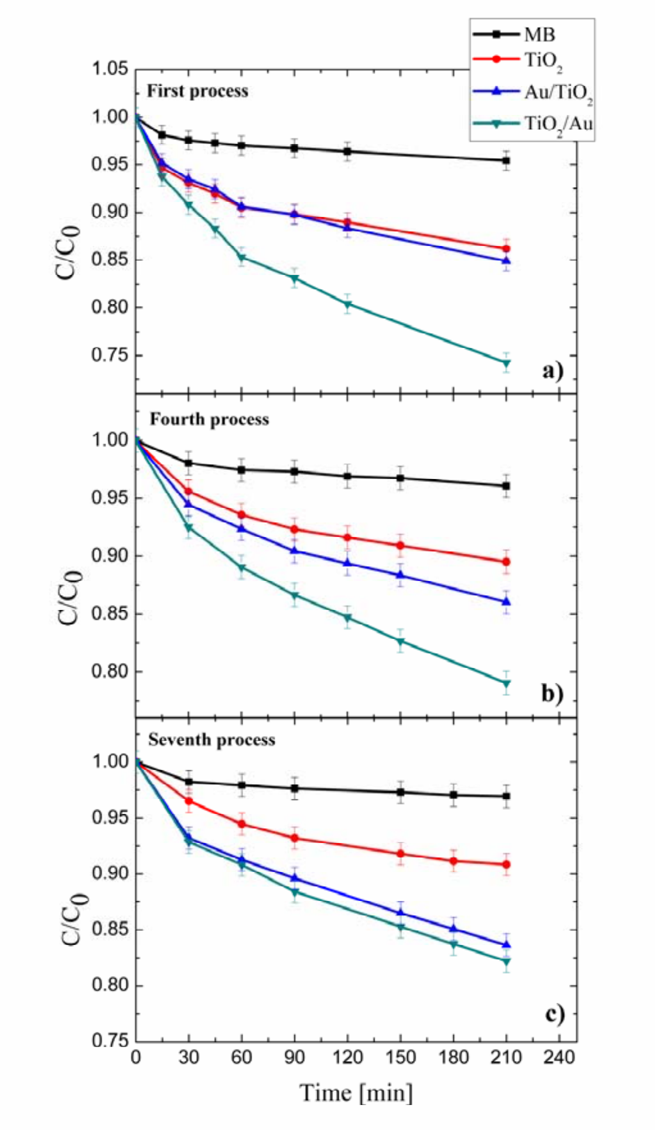

Figure 4: MB degradation under UV-irradiation for four samples: MB (squares), MB with the TiO_2 flat film (circles), MB with the Au/TiO_2 sample (triangles) and MB with the TiO_2/Au sample (diamonds). The results for the (a) first, (b) fourth and (c) seventh photo-degradation process are reported.

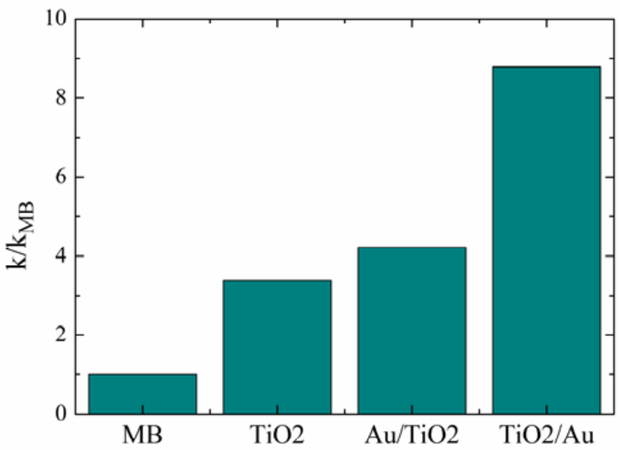

Figure 5: Photo-degradation reaction rate, normalized to the value obtained for the MB in the absence of catalyst, for the different investigated samples: TiO_2 flat film, Au/TiO_2 and TiO_2/Au.

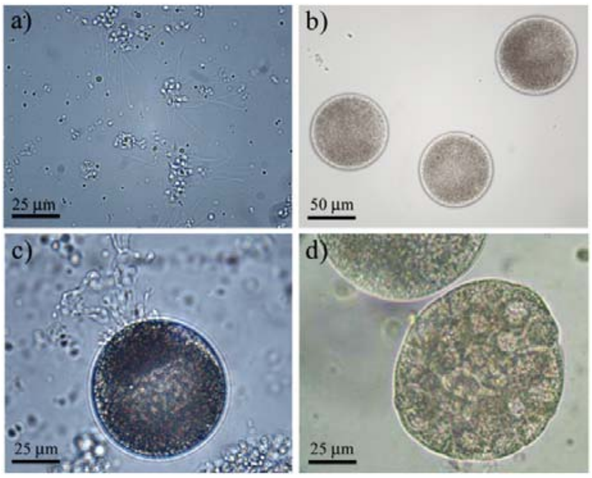

Figure 6: Reproductive cycle of *Mytilus galloprovincialis*: a) sperms after 10 min; b) unfertilized eggs after 10 min; c) fertilized eggs after 15 min; d) blastulae after 24 h.